1-1-2013

A geospatial assessment of the relationship between reef flat community calcium carbonate production and wave energy

S M. Hamylton
University of Wollongong, shamylto@uow.edu.au

A Pescud
University of Wollongong, ap980@uowmail.edu.au

J X. Leon
University of Queensland

D Callaghan
University of Queensland

A geospatial assessment of the relationship between reef flat community calcium carbonate production and wave energy

Abstract

The ability of benthic communities inhabiting coral reefs to produce calcium carbonate underpins the development of reef platforms and associated sedimentary landforms, as well as the fixation of inorganic carbon and buffering of diurnal pH fluctuations in ocean surface waters. Quantification of the relationship between reef flat community calcium carbonate production and wave energy provides an empirical basis for understanding and managing this functionally important process. This study employs geospatial techniques across the reef platform at Lizard Island, Great Barrier Reef, to (1) map the distribution and estimate the total magnitude of reef community carbonate production and (2) empirically ascertain the influence of wave energy on community carbonate production. A World-View-2 satellite image and a field data set of 364 ground referencing points are employed, along with data on physical reef characteristics (e.g. bathymetry, rugosity) to map and validate the spatial distribution of the four major community carbonate producers (live coral, carbonate sand, green calcareous macroalgae and encrusting calcified algae) across the reef platform. Carbonate production is estimated for the complete reef platform from the composition of these community components. A synoptic model of wave energy is developed using the Simulating WAves Nearshore (SWAN) two-dimensional model for the entire reef platform. The relationship between locally derived measures of carbonate production and wave energy is evaluated at both the global scale and local scale along spatial gradients of wave energy traversing the reef platform. A wave energy threshold is identified, below which carbonate production levels appear to increase with wave energy and above which mechanical forcing reduces community production. This implies an optimal set of hydrodynamic conditions characterized by wave energy levels of approximately 300 J m−2, providing an empirical basis for management of potential changes in community carbonate production associated with climate change-driven increases in wave energy.

Keywords

wave, production, carbonate, calcium, energy, between, community, assessment, geospatial, flat, relationship, reef

Disciplines

Medicine and Health Sciences | Social and Behavioral Sciences

Publication Details

Hamylton, S., Pescud, A., Leon, J. X. and Callaghan, D. (2013). A geospatial assessment of the relationship between reef flat community calcium carbonate production and wave energy. Coral Reefs, 32 (4), 1025-1039.

A geospatial assessment of the relationship between reef flat community calcium carbonate production and wave energy

S. Hamylton[1], A. Pescud[1], J.X. Leon[2] and D.P. Callaghan[3]

[1]*School of Earth and Environmental Sciences, University of Wollongong, Australia, NSW2522.*

[2]*Global Change Institute, University of Queensland, Brisbane, Queensland, 4072, Australia.*

[3]*School of Civil Engineering, University of Queensland, Brisbane, Queensland, 4072, Australia.*

Email: sarah_hamylton@uow.edu.au

Tel: +61 42213589

Abstract

The ability of benthic communities inhabiting coral reefs to produce calcium carbonate underpins the development of reef platforms and associated sedimentary landforms, as well as the fixation of inorganic carbon and buffering of diurnal pH fluctuations in ocean surface waters. Quantification of the relationship between reef flat community calcium carbonate production and wave energy provides an empirical basis for understanding and managing this functionally important process. This study employs geospatial techniques across the reef platform at Lizard Island, Great Barrier Reef to (i) map the distribution and estimate the total magnitude of reef community carbonate production, and (ii) empirically ascertain the influence of wave energy on community carbonate production. A World-View-2 satellite image and a field dataset of 364 ground referencing points are employed, along with data on physical reef characteristics (e.g., bathymetry, rugosity) to map and validate the spatial distribution of the four major community carbonate producers (live coral, carbonate sand, green calcareous macroalgae and encrusting calcified algae) across the reef platform. Carbonate production is estimated from the composition of these community components for the complete reef platform. A synoptic model of wave energy is developed using the **S**imulating **WA**ves **N**earshore (SWAN) two-dimensional model for the entire reef platform. The relationship between locally derived measures of carbonate production and wave energy is evaluated at both the global scale and local scale along spatial gradients of wave energy traversing the reef platform. A wave energy threshold is identified, below which carbonate production levels appear to increase with wave energy and above which mechanical forcing reduces community production. This implies an optimal set of hydrodynamic conditions characterized by wave energy levels of approximately 300Jm^{-2}, providing an empirical basis for management of potential changes in community carbonate production associated with climate change driven increases in wave energy.

Remote sensing, bathymetry, rugosity, calcification

Introduction

Benthic communities precipitate calcium carbonate ($CaCO_3$) via light-enhanced calcification whereby calcium and carbonate ions derived from seawater are converted into calcium carbonate (Kinzie and Buddemeier 1996). Active growth of calcifying organisms is functionally important because it leads to the build up of substantial carbonate reef framework and associated sedimentary landforms (Kench 2011) and mediates the chemical composition of oceanic waters through the fixation of carbon and associated pH buffering (Kleypas and Langdon 2006). Coral reef platforms can be subdivided into 5 morphological zones: forereef, reef crest, reef flat, back reef and lagoon (Hopley et al. 2007) within which the different benthic assemblages make a statistically distinct contribution to reef framework construction. Major carbonate producers include scleractinian corals, coralline algae, green calcified algae, molluscs and benthic foraminifera (Montaggioni and Braithwaite 2009). Overall community carbonate production can be estimated using census-based approaches that sum across the contribution made by each of the individual benthic community components based on areal coverage of each reef organism and their characteristic production rates, which are established by taking measurements either *in-situ* or in a laboratory setting (Harney and Fletcher 2003).

Carbonate-producing benthic assemblages are spatially structured along gradients of localized environmental controls which are discernable within the wider context of the reef system, such as water depth, incident wave energy, temperature, degree of aragonite saturation, nutrient levels and suspended particulate organic matter (Montaggioni and Braithwaite 2009). Several studies have suggested the existence of a relationship between carbonate production and water movement. Such observations have been made at spatial scales ranging from the preferential alignment of live coral polyps with wave scour, producing resistant reef spurs orientated toward high energy coastlines (Shinn 1966), to the geographical structuring of reef ecological zones based on wave exposure (Geister 1977), to the tendency for reef platforms to become more developed on windward as opposed to leeward island aspects (Lugo-Fernandez and Roberts 2011). Underpinning these observations is the enhancement of carbonate production by water movement through the circulation of nutrients and removal of metabolic waste products in high-energy environments (Atkinson and Bilger 1992; Atkinson et al. 1994; Hearn et al. 2001). Notwithstanding highly energetic environments, the enhancing effects of circulation on carbonate production often appear to outweigh potential destructive effects of mechanical erosion, possibly due to the selection of stress tolerant growth morphologies such as massive corals and the stability afforded by associated community components such as encrusting calcified algae in high energy environments (Done 2011).

The development of remote sensing technology has yielded valuable information in the form of higher specification (accuracy, precision), synoptic (~150km^2) satellite images. These afford the opportunity to simulate the distribution of carbonate production units across entire reef systems and draw new comparisons of reef biogeochemical performance in space. To this end, census based local estimates of production have been successfully scaled up by applying image classifying remote sensing datasets to estimate carbonate production across complete reef systems (Andréfouët and Payri 2000; Vecsei 2001, 2004; Moses et al. 2009; Leon and Woodroffe 2013). Predictive mapping of benthic cover offers an alternative approach whereby statistical models draw on species-environment relationships to simulate the geographical distribution of a given species. Such an approach establishes statistical links between spatially continuous information, usually derived from remote sensing datasets, on physical environmental drivers (e.g., bathymetry, rugosity) and point samples of benthic cover. This statistical relationship is subsequently used to extrapolate predictions of benthic cover over larger spatial scales (Guisan and Zimmerman 2000; Brown et al. 2011). The result is a map that predicts the cover of individual benthic components (e.g., live coral, coralline algae etc.) at a ratio level of measurement across the entire reef system. By combining a set of predictive maps relating to the different carbonate producing components of the benthic community, it is possible to model the spatial distribution of overall community carbonate production across the entire reef platform using census-based estimations.

It is possible to compare two variables across different environmental settings by identifying and interrogating meaningful spatial gradients across broad scales (e.g., 1 – 100 km^2) (Haining 2003).

This principles applies across different reef platform locations (e.g. forereef vs. lagoon), which give rise to different levels of wave energy. Varying the distance from point sources of input (e.g., incident wave impact on the seaward reef crest) in this manner therefore permits exploration of how this variable influences carbonate production. The objective of this study is to generate synoptic representations of both overall community carbonate production and levels of incident wave energy across the reef flat at Lizard Island in order to conduct a geospatial assessment of the empirical relationship between the two. The geospatial assessment will be conducted at both the global scale, that is, making simultaneous use of all sample data within the reef flat area and also at the local scale along defined transects that span observable wave energy gradients. The advantage of using a multi-scale approach is that both stationary (i.e., homogeneous) and non-stationary relationships can be tested (Fortin and Dale 2005). To the authors' knowledge, the relationship between local measures of carbonate production and wave energy has not been assessed in this manner before.

Study area

The Lizard Island group is a series of three granitic islands located approximately 30km off the northern Queensland coastline, including the main island to the north, Lizard Island (395 m altitude) and the smaller Palfrey and South Islands to the south (Fig. 1). A complex of reefs developed around these continental island foundations during the Holocene, including a narrow fringing reef around much of the Main Island and broader barrier reefs connecting Lizard Island to South Island and Palfrey Island to South Island. These crescentic reefs enclose a lagoon that is up to 10 m deep. The reef flat within the Lizard Island group falls primarily within the three islands and is bordered along the southeastern facing windward aspect by the barrier reef, a series of reef patches in the west and a narrower fringing reef rim around the northeastern boundary of Lizard Island itself.

Previous studies of the Lizard Island reef flat have published in-situ measurements of carbonate production across a range of benthic substrates, including the coral rich outer reef flat, and the sand, coral and algal dominated central and leeward sections of the reef flat (LIMER 1975), the coral-algal dominated shallow seaward reef flat, the algal pavement and the protected lagoon environment (Smith and Kinsey 1976), the large benthic foraminifer depositions (Smith and Weibe 1977) and the encrusting calcified algae (Chisholm 2000). These range from 1 – 4.5 kg $CaCO_3$ m^{-2} yr^{-1} and are in broad agreement with results obtained from regional carbonate production studies on the Great Barrier Reef, which appear to converge around a set of standard values (Kinsey 1985; Hopley et al. 2007). They are also comparable with rates derived from three cores recovered that provide a record of past Holocene reef growth on the windward reef (Rees et al. 2006).

This study focuses on the four key carbonate producers present on Lizard Island reef flat, which have been identified as live coral, carbonate sand, green calcareous macroalgae and encrusting calcified algae (Kinsey and Davies 1975, Fig. 2). Much of the live coral is present along the reef flat / reef crest boundary, particularly along the eastern facing coastlines but also in association with algae along the shallow (<2m water depth) southeastern reef flat (Pichon and Morrisey 1981). Large beds of calcareous *Halimeda* macroalgae inhabit the lagoon floor (Nelson 1992), while encrusting calcified algae dominate much of the windward reef crest (Chisholm 2000) Carbonate sand appears to have largely been deposited along the inner eastern reef flat margin.

Materials and methods

The study used predictive benthic cover mapping to generate an overall model of community carbonate production across the whole Lizard Island reef platform. Wave energy was then modeled using the **S**imulating **WA**ves **N**earshore (SWAN) two-dimensional model for the entire reef platform An empirical assessment of the relationship between community carbonate production and wave energy was then conducted at both the global and local scale (Fig. 3).

Census- Based Estimation of carbonate production

Collection of in-situ field information

To generate and validate the census-based estimate of overall reef community carbonate production, a series of 642 (364 for generation and 278 for validation) *in situ* video snapshots were collected from the 7th- 17th December 2011 to sample the benthic communities inhabiting the reef platform around Lizard Island (see Fig. 1). At each sample point, an underwater video camera was lowered on a cable from a boat and held so that it drifted approximately 50 cm above the sea floor. With the boat as close to a stationary position as possible, a 30 second oblique video snapshot was taken and the geographical position of each video snapshot was recorded using a GPS. This field survey method enabled a representative range of reef community assemblages to be sampled across a large geographical area to support further estimation of carbonate production rates.

All video snapshots were individually viewed and the percentage cover of each benthic component was recorded, including major carbonate producers live coral, carbonate sand, green calcareous macroalgae and encrusting calcified algae. Gross calcium carbonate production for each video sample site was estimated using a census-based approach (Harney and Fletcher 2003; Perry et al. 2012). For each video sample, published production values (P_i) of each benthic component (see Table 1) were converted to gross production, G_c, by multiplying by the proportion of carbonate-producing biotic components that made up the characteristic assemblages (% cover) and summing across the total number (n) of biotic components:

$$G_c = 0.01 \times \sum_{i=1}^{n} (P_i \times \%\text{cov}er) \qquad (1)$$

Mapping benthic cover of the four major carbonate producers (live coral, carbonate sand, green calcareous macroalgae and encrusting calcified algae)

A predictive habitat mapping approach (Guisan and Zimmerman 2000; Brown et al. 2011) was employed to map the distribution of the four major carbonate producing benthic components (live coral, carbonate sand, green calcareous macroalgae and encrusting calcified algae). For the set of 364 video sample points, this established a statistical relationship between the cover of each benthic component and a series of independent physical variables across the reef platform (Hamylton et al. 2012). Independent variables included remotely sensed benthic reflectance extracted from a WorldView-2 satellite image of the reef platform (bands 1-4), a digital elevation model (DEM) of the reef platform (Leon et al. 2013) and a series of benthic terrain variables derived from the DEM including slope, bathymetric position index, terrain rugosity and elevation variety. The horizontal resolution of the DEM was 2m and the vertical accuracy was 0.45m. Table 2 summarises the source and derivation of each of the independent physical variables.

A spatially explicit regression model was used to predict the distribution of live coral, carbonate sand, green calcareous macroalgae and encrusting calcified algae on the basis of the independent physical variables around Lizard Island following a methodology that has been used successfully to model reef community composition in the Red Sea (Hamylton 2011). A spatial error model was employed that subdivided the error component of the regression model into spatially structured unexplained and unexplained components. The spatially structured unexplained component was then modeled as a simultaneous spatially autocorrelated parameter using a maximum likelihood procedure (Smirnov and Anselin 2001). Values for the independent variables were extracted and regressed against the percentage of each benthic component recorded for each of the video sampling point records. Different combinations of the independent physical variables listed in Table 2 were iteratively tested using the GeoDa software package in a spatial error regression model and combinations that gave a statistically significant regression results (R^2>0.7) were retained for each benthic cover.

Beta coefficient diagnostics were established for the combination of independent variables associated with each significant model from the 364 sample locations and used to generate a continuous, synoptic prediction map of the distribution of each benthic cover type around Lizard Island. The spatial error regression model was specified by combining the beta coefficients with raster datasets representing the independent variables using the Model Builder and Raster Calculator tools of ArcGIS10. Different combinations of variables were employed for each benthic cover type.

To validate each benthic component model, the predicted values from the regression analysis were plotted against the set of 278 independent observations of the percentage of each benthic cover type. The coefficient of determination (R^2) assessed the correspondence between the two datasets.

Mapping overall community carbonate production

The carbonate production distribution map was derived by combining the individual benthic component maps using the assumption that the sum of carbonate production from all benthic components is equal to that of the whole community (Andréfouët and Payri 2000). As with the video samples, each benthic component layer was weighted in accordance with the carbonate production rate (Equation 1). Cumulative error was calculated by summing the proportion of variation that remained unexplained by each spatial error model of benthic cover. This was then expressed as a fraction of the mean production value of the overall community carbonate production.

The carbonate production map was validated against an independent field dataset of 278 video footage samples from which point estimates of community carbonate production were derived (Equation 1) using rank correlation methods (Kendall and Gibbons 1990). Observed and modelled carbonate production values were ranked and compared using a general correlation coefficient (Equation 2). This yielded a metric that indicated the amount of agreement between the rankings across a scale that ranged from 1 (perfect correlation between rankings) to -1 (perfect negative correlation between the rankings).

$$\Gamma = \frac{\sum_{ii,j=1}^{n} a_{ij} b_{ij}}{\sqrt{\sum_{ii,j=1}^{n} {a_{ij}}^2 \sum_{ii,j=1}^{n} {b_{ij}}^2}} \quad (2)$$

Where a_{ij} = rank value for sample population 1 for the ith and jth pair of individuals
b_{ij} = rank value for sample population 2 for the ith and jth pair of individuals
n =number of points in sample population

Mapping wave energy across the reef platform

The **S**imulating **WA**ves **N**earshore (SWAN) two-dimensional model was employed to estimate wave generation and propagation in the horizontal plane (Booij 1999; Holthuijsen 2007; Ris, 1999). A series of spatial wave parameters was generated from wind measurements across Lizard Island, including significant wave height H_{RMS}, mean wave period T_m and peak wave energy direction θ_p. Of these, oscillatory motion at the seabed was selected as the parameter of relevance for comparison to benthic community calcification. SWAN solved the oscillatory wave hydrodynamics in parametric form using the wave action flux conservation equation. Consequently, SWAN includes predictions of wave hydrodynamics and includes sink (e.g., wave breaking, bottom friction) and source (e.g., wave generation and wave-wave interaction) terms.

Wave shoaling and refraction mechanisms are included in SWAN (Holthuijsen, 2007). To correct for the 2 m tidal fluctuation at Lizard Island, Navy Seafarer tidal predictions were obtained, which were compared to measurements taken in situ and confirmed as acceptable.

The wave frequency spectrum was modeled in the range 0.125 Hz through to 2 Hz (periods ranging between 0.5 s to 8s) and the wave directions included were ±90º relative to the wind direction. Bottom friction, triad and quadruplet wave-wave interactions and depth-limited breaking were included along with an approximate wave diffraction method (Holthuijsen, 2003). The model applied the enhanced convergent test proposed by (Zijlema and van der Westhuysen, 2005) and incorporated improvements for simulating waves in fetch-limited lagoons (Van der Westhuysen, 2010).

The wave propagation model consisted of six nested grids at a series of resolution increments (1.3 km, 0.9 km, 0.53 km, 178 m, 61 m and 21 m) respectively, all being rotated at 45 ° in a CCW direction from grid north. A high-resolution grid was required to resolve wave dissipation (wave breaking and other dissipation mechanics), wave shoaling and refraction processes that can intensify when waves propagate through water depths that are less than twice their wavelength (Dean, 1991; Nielsen, 2009). The model comprised approximately 50 million computational points and incorporated coarse bathymetry at the regional scale, i.e. within a grid area of 17,500sq.km (Beaman, 2010) and finer scale bathymetry collected in-situ over the reef platform (see previous section on collection of in-situ field information).

A look up table approach was adopted whereby the model was run for a series of constant wind speed, direction and tide level combinations to form a numerical transfer function. Linear interpolation was used when converting the measured wind and tide inputs into wave parameters.

To validate this approach, the spatial distribution of the resultant significant wave height model parameter was validated compared against published values of in-situ wave power measurements for the Coconut Beach section of the Lizard Island reef flat (Daly, 2005; Ford, 2010). Water surface elevation measurements were taken during two separate periods of fieldwork using 4 pressure sensors across 4 days in May 2005 (Daly, 2005) and 25 days during May-June 2006 (Ford, 2010). Average significant wave height measurements from 8 sites across the reef flat were compared with those modeled for the same months via linear regression.

Empirically evaluating the relationship between carbonate production and wave energy

The relationship between carbonate production and wave energy was assessed through extraction and comparison of co-located measurements of both carbonate production and wave energy at both the global scale and at the local scale. For the global assessment, the properties of carbonate production and wave energy were assumed to be independent of absolute location and direction in space and a shapefile of 23,605 points in a grid was generated that covered the entire reef flat area. An appropriate grid spacing of 3 m intervals was determined by inserting carbonate production values for all the points of the high resolution raster model into a semivariogram and reading off the sill point at which spatial dependency between neighbouring points no longer existed (Haining 2003). In the first instance, all points were plotted against each other to investigate the overall relationship. In the second instance, the grid point data were subset into wave energy ranges using spatial and attribute queries and the collective statistics (mean, cumulative error, range) of these subsets were compared using box plots.

For the local scale assessment, three transects were established that crossed the reef platform profile and traversed wave energy gradients. Data on carbonate production and wave energy were extracted at 3 m intervals along these transects and plotted against each other to ascertain the nature of the relationship between the two. A profile of modeled carbonate production values across the different geomorphological zones at Lizard Island (inner reef flat, lagoon, outer reef flat and reef crest) was also generated for visual assessment.

Results

Mapping carbonate production

Each of the predictive benthic component distribution models for live coral, carbonate sand, green calcareous macroalgae and encrusting calcified algae produced a statistically significant result ($p < 0.001$), providing a basis for rejecting the null hypothesis that each combination of explanatory variables had no influence on the observed distribution of benthic components. Validations against field data indicated a high correspondence between modelled and observed benthic cover (R^2 ranged from 0.79 – 0.91) (Fig. 4).

The predictive distribution maps indicated that live coral dominated the eastern fringe of Lizard Island's reef system, particularly around the southeastern reef crest and slope with the development of patch reefs around the lagoon and across the leeward reef flat (Fig. 4a). Carbonate sand (Fig. 4b) dominated the shallow areas proximal to the shoreline and along the windward and leeward reef flat. A dense cover of green calcareous macroalgae (Fig. 4c) was predicted in the lagoon and on the deeper westerly side of the leeward reef flat, with minimal cover in the shallow regions of the windward and leeward reef flats. The distribution of encrusting calcified algae (Fig. 4d) appeared to be limited to the easterly fringes of the reef system.

Figure 5 illustrates the modelled distribution of overall reef community carbonate production, for which the rank correlation coefficient indicated a high correspondence with video sample rankings ($\Gamma = 0.81$). Total modelled calcium carbonate production for the community ranged from 0 to 3.00 kg $CaCO_3$ m^{-2} yr^{-1} and indicated a spatial distribution in which the highest production values fell on the northeasterly and southeasterly fringes of the reef system. The lagoon showed relatively high values of production compared to the surrounding reef flats. Along the windward reef flat, high production values tended to taper off to lower values along a northwesterly trajectory. Low values of carbonate production were indicated along the leeward reef flat with the occasional high value for patch reefs. The most westerly areas off the leeward reef flat revealed moderate carbonate production values. Cumulative error associated with these estimates of carbonate production was ±0.21 $kgCaCO_3m^{-2}yr^{-1}$.

Empirically evaluating the relationship between carbonate production and wave energy

The SWAN wave energy model indicated a hydrodynamic regime that was dominated by the southeast trade winds, the spatial distribution of which corresponded with available data on significant wave heights (R^2=0.88) (Fig. 6).

The global plot of carbonate production against wave energy for the complete grid of 23605 sample points revealed a weak linear trend (R^2 = 0.19), with values ranging from 0.72 – 3.36 kg $CaCO_3$ m^{-2} yr^{-1}. Figure 7 illustrates the box plot of the distribution of carbonate production across wave energy regimes. Mean carbonate production (±cumulative error) in low energy zones (100-140 J/m^2) was 1.44 (±0.105) kg $CaCO_3$ m^{-2} yr^{-1}, which was lower than that calculated in the high wave energy zones (380-420 J/m^2) that produced a mean of 2.15 (±0.105) kg $CaCO_3$ m^{-2} yr^{-1}. The difference between these zones was therefore meaningful when the cumulative error associated with the individual benthic cover models was taken into account.

The local scale evaluations along each of the wave energy transects revealed similar relationships between carbonate production and wave energy for different profiles across the reef platform (Figs. 6 and 8). Transect 1 traversed the fringing reef profile and indicated a relationship that was best characterized as a second order polynomial function (R^2 0.73). Transects 2 and 3 traversed the entire reef platform from the windward slope, across the lagoon to the inner leeward shore. Trends across these zones were also characterized by a second order polynomial function (Transect 3 R^2 = 0.78, Transect 2 R^2 = 0.77). These functions indicated an initial increase in carbonate production with wave energy to a point, coinciding with a seabed orbital velocity of approximately 0.55ms^{-1}, or an energy density of 300 $J/m^2/yr^{-1}$, at which carbonate production started to decrease.

Observable trends in localized measures of carbonate production across three transects traversing different geomorphological zones of the reef platform are illustrated in Figure 9. Transect 1 illustrates a general increase in production moving across the reef platform towards the reef crest. Transects 2 and 3 indicate lower values of carbonate production on the inner reef flat closer to Lizard Island with moderate production values across the lagoon that display a gradual increase approaching the outer reef. Lower production values are apparent on the outer reef flat in areas of sand deposition and the highest production values were observed on the southeastern reef crest.

Discussion

The main aims of this study were to employ geospatial techniques across the Lizard Island reef to *(i)* estimate total reef community carbonate production invoking census based principles in a manner not previously employed, and *(ii)* empirically ascertain the influence of wave energy on community carbonate production. In relation to the first aim, predictive distribution models were generated for the individual benthic components of live coral, carbonate sand, green calcareous macroalgae and encrusting calcified algae. The spatial error models captured a large proportion of the variation observed in the field datasets for these benthic components (R^2 ranged from 0.79 to 0.91). This procedure yielded spatially extensive predictions of benthic cover that extended the previous localized studies on the distribution and zonation of benthic communities at Lizard

Island (Pichon and Morrissey 1981; Nelson 1992). It is difficult to ascertain the extent to which the combination of these predictions allowed an accurate estimate of community carbonate production to be reached. Modelled community carbonate production values ranged from 0 to 3.82 kg$CaCO_3$ m^{-2} yr^{-1}, with a mean overall carbonate production value of 1.84 (±0.21) kg$CaCO_3$ $m^{-2}yr^{-1}$. This was comparable to the value of 1.81 kg$CaCO_3$ m^{-2} yr^{-1} estimated for the complete reef system using hydrochemical alkalinity reduction methods (LIMER 1975; Kinsey 1985). Elsewhere, census-based methods have yielded similar estimates of overall reef system community carbonate production, for example 1.15 kg $CaCO_3$ m^{-2} yr^{-1} at St Croix in the US Virgin Islands (Hubbard et al. 1990) and 1.66 kg $CaCO_3$ m^{-2} yr^{-1} in the Torres Strait (Hart and Kench 2007).

While the use of remote sensing datasets for estimating carbonate production is not a new phenomenon, the manipulation of these datasets in the predictive mapping manner demonstrated here represents a new approach to the implementation of the census-based methodology. The predictive statistical extrapolations provided a quantitative measurement of benthic cover for each individual component of the carbonate census, which was subsequently weighted by the production rate and summed to estimate community production. This represents a fundamentally different type of information to that generated using standard remote sensing approaches, which assign a pixel to one single cover type over a nominal ground area (Andréfouët & Payri 2000; Vecsei, 2001, 2004; Moses et al. 2009). In doing so, the predictive mapping approach allows a more realistic characterization of the mixture of carbonate producing assemblages that co-exist on reef platforms (Montaggioni and Braithwaite 2009), as well as lending more versatility to subsequent modeling exercises through the provision of information at a higher measurement level (i.e., ratio as opposed to nominal) (Haining 2003).

The spatial distribution of overall community carbonate production around the reef platform suggested that different geomorphological units were associated with distinct community assemblages, resulting in zonation of carbonate production (see Fig. 9). For example, the eastern windward forereef was identified as a productive area because of the high proportion of live coral found here. Likewise, the presence of green calcareous macroalagae in the lagoon and around the deeper western platform shelf corresponded to a relatively high productivity environment (0.9 – 2.1 kg $CaCO_3$ m^{-2} yr^{-1}). Similar findings have been recorded at Pico Feo lagoon in Panama where dense beds of *Halimeda Incrassata* dominate the lagoonal setting with an estimated production of 2.3 kg $CaCO_3$ m^{-2} yr^{-1} (Freile and Hillis 1997).

In relation to the second aim, a positive association was revealed between carbonate production and wave energy levels across the reef platform, as initially hypothesized. This can be seen at both the global scale, with significant differences observed across the different wave energy zones (Fig. 7) and also along the reef platform transects. In the case of reef platform transects 2 and 3, this relationship appeared to break down above a seabed orbital velocity of 0.55ms^{-1}wave energy density level of approximately 300 Jm^{-2}, beyond which a negative association was discernable. This relationship, characterized here with a second order polynomial function, can likely be explained by variation in the influence of hydrodynamics at different energy levels. At low energy levels, the transport of nutrients and removal of metabolic wastes enhance carbonate production (Hearn et al. 2001; Veron 2011), however, at higher energy levels the mechanical forcing results in a transition in community composition that favours more stress tolerant growth forms, such as encrusting and massive corals, and encrusting algae (Massel 2005). While the cover of community components like coral may remain high, these stress-tolerant growth forms calcify at a lower rate and, with an associated increase in the proportion of encrusting calcified algae which also calcifies at a comparatively low rate, this decreases total community carbonate production. Such a transition is evident in the increasing percent cover of encrusting calcified algae in high wave energy environments (Figure 8). Similar changes in community structure associated with high energy zones have been noted in the form of algal ridges on the seaward aspect of many Caribbean reefs (Geister 1977; Macintyre et al. 2001). While this competing influence at different wave energy levels has long been stipulated (e.g., Davis 1976), the empirical approach employed in the present study permits identification of a consistent wave energy threshold at which the metabolic benefits of increased water movement are optimal for the different benthic carbonate producers.

The term eco-morphodynamics refers to the interaction and co-adjustment of physical and ecological processes that is mediated by calcium carbonate production, transfer and deposition within a coral reef system (Kench 2011). Eco-morphodynamics provides a valuable framework for understanding how global change factors, such as atmospheric, ocean and anthropogenic forcing influence biological and physical processes, such as carbonate production and wave energy and how these, in turn, drive geomorphological processes in coral reef systems, such as Holocene reef growth, carbonate cycling, sediment transport and deposition (Kench et al. 2009). Within this framework, the practical value of an empirical assessment of the relationship between wave energy and carbonate becomes evident. For example, the existing wave energy model suggests an annual mean energy level across the reef platform of 262 Jm^{-2} (standard deviation 84 Jm^{-2}) and given information on anticipated changes in wave energy, for example, a 2% increase in energy levels by 2100 (CSIRO 2007), the identified empirical threshold of 300 Jm^{-2} can be used to quantify potential reductions in overall community carbonate production and identify locations where these may occur due to the wave energy threshold being exceeded. In turn, this could guide the implementation of practical coastal management initiatives such as the introduction of breakwaters, to reduce extreme levels of wave energy where they may have a deleterious influence on carbonate production.

The important contribution of benthic foraminifera was excluded from the community carbonate production levels modeled in this study as they were too small to be identified in the video footage. Net rates of calcification by the benthic foraminifera *Marginopora vertebralis* on Lizard Island reef flat have been estimated to be approximately 0.26 kg $CaCO_3$ m^{-2} yr^{-1} when accounting for dissolution (LIMER 1975; Smith and Wiebe 1977). At nearby Green Island cay, foraminifera were found to be the single most important contributor to the sediment mass of the Island, with production rates of 0.48 ± 0.28 kgCaCO3 m^{-2} yr^{-1} for *Amphistegina lessonii*, *Baculogypsina sphaerulata*, and *Calcarina hispida* inhabiting the algal reef flat making a fundamental contribution to the development and maintenance of a coral sand cay (Yamano et al. 2000). Similarly, estimations based on measured growth rates, overall occupation of reef flat turf algae habitat and population densities of *Marginopora vertebralis* and *Baculogypsina sphaerulata* at One Tree Island suggested annual $CaCO_3$ production of 71.7 x 10^3 g m^{-2} yr^{-1} and 2.86 x 10^3 g m^{-2} yr^{-1} respectively (Doo et al. 2013). Such potential contributions warrant further investigation and it is recommended that further census-based studies into carbonate production at Lizard Island should adopt a field sampling technique that incorporates this potentially important component of the carbonate budget.

The present study considers only the constructional processes and excludes the biological and physical destructive processes that define the overall carbonate budget, the end result of which in turn determines functional outcomes such as reef growth and island development. While the scope of this study was to quantify overall community carbonate production and empirically evaluate its relationship to wave energy, a more complete understanding of the functional importance of this production can be reached through determination of a comprehensive carbonate budget (Mallela and Perry 2007; Perry et al. 2012). At Lizard Island, the basis for parameterising such a budget has been provided through research into overall community bioerosion rates of primary and secondary reef framework (Kiene and Hutchings 1992, 1994), including erosion by parrotfish (Bellwood 1995a, 1995b, 1996) and endolithic borers (Trillobet and Golubic 2005) and the export of coral fragments along the margins of reefs (Hughes 1999).

In summary, two identifiable outcomes of this study advance our understanding of reef flat community calcium carbonate production and its relationship to wave energy. Firstly, a new methodological approach is presented that allows census-based estimations of community carbonate productions to be made in a manner not previously used before. Comparison against hydrochemically-derived estimates indicates that this approach holds promise for a more realistic characterization of the mixture of carbonate producing assemblages that occupy reef platforms than has hitherto been the case. Secondly, the empirical evaluation of the relationship between community carbonate production enabled the identification of a collective wave energy threshold at which the metabolic benefits of increased water movement are optimal for the different benthic carbonate producers. This offers a quantitative verification of previous suggestions about the tradeoff between metabolic advantages and mechanical disadvantages of water movement. While this study could profitably be improved by the inclusion of the contribution of foraminiferal carbonate production and an extension of the analysis to destructive processes such as bioerosion and mechanical forcing, these two points nevertheless extend our understanding of reef flat community calcium carbonate production and its relationship to wave energy.

Acknowledgements

This work would not have been possible without the support of a Lizard Island Research Station Fellowship grant, 2011 and a University of Wollongong URC grant, 2011 awarded to SH. JL's contribution was funded by a UQ start-up grant and an Australian Research Council SuperScience Fellowship grant (FS100100024). Professor Colin Woodroffe and Dr Valerie Harwood are thanked for assistance with fieldwork.

References

Andréfouët S, Payri C (2000) Scaling-up carbon and carbonate metabolism of coral reefs using in-situ data and remote sensing. Coral Reefs 19:259-269

Atkinson MJ, Bilger RW (1992) Effects of water velocity on phosphate uptake on coral reefs. Limnol Oceanogr 37:261-272

Atkinson MJ, Kotler E, Newton P (1994) Effects of water velocity on respiration, calcification and ammonium uptake in a *Porites compressa* community. Pac Sci 48:296-303

Beaman, RJ (2010) Project 3DGBR: A high-resolution depth model for the Great Barrier Reef and Coral Sea. Cairns, Australia: Marine and Tropical Sciences Research Facility, Project 2.5i.1a Final Report, 13pp.

Booij, N, Ris, RC, Holthuijsen, LH (1999) A third-generation wave model for coastal regions 1. model description and validation. J Geophys Res 104:7649-7666

Bellwood DR (1995a) Carbonate transport and within-reef patterns of bioerosion and sediment release by parrotfishes (family Scaridae) on the Great Barrier Reef. Mar Ecol Prog Ser 117:127-136

Bellwood DR (1995b) Direct estimate of bioerosion by two parrotfish species, *Chlorurus gibbus* and *C. sordidus*, on the Great Barrier Reef. Aust Mar Biol 121:419-429

Bellwood DR (1996) Production and reworking of sediment by parrotfishes (family *Scaridae*) on the Great Barrier Reef. Mar Biol 125:795-800

Boucher G, Clavier J, Hily C and Gattuso JP (1998) Contribution of soft-bottoms to the community metabolism (primary production and calcification) of a barrier reef flat (Moorea, French Polynesia). J Exp Mar Biol Ecol 225:269-283

Brown CJ, Smith SJ, Lawton P, Anderson JT (2011) Benthic habitat mapping: A review of progress towards improved understanding of the spatial ecology of the seafloor using acoustic techniques. Estuar Coast Shelf Sci 92:502-520

Chisholm JRM (2000) Calcification by crustose coralline algae on the northern Great Barrier Reef, Australia. Limnol Oceanogr 45:1476-1484

CSIRO & Bureau of Meteorology (2007) Climate change in Australia: Technical Report. Available for download at: http://www.climatechangeinaustralia.gov.au/technical_report.php

Daly M (2005) Wave energy and shoreline response on a fringing reef complex, Lizard Island, Qld, Australia. B Env Sci thesis, University of New South Wales, p105

Davis WM (1976) The coral reef problem. American Geographical Society, New York

Dean RG, Dalrymple, RA (1991) Water wave mechanics for engineers and scientists. World Scientific, Singapore

Done T (2011) Coral reef, definition. In: Hopley, D (ed) Encyclopedia of modern coral reefs: Structure form and process. Springer, Berlin, pp 261-267

Doo S, Hamylton S, Byrne M (2013) Reef scale assessment of Large Benthic Foraminifera populations on One Tree reef and future carbonate production potential in a warming ocean. Zool Stud 'in press'

Ford MR (2010) Sedimentological implications of durability and physical taphonomic processes on a fringing reef, Lizard Island, Australia. PhD Thesis, University of Auckland

Fortin M, Dale MRT (2005) Spatial analysis: A guide for ecologists. Cambridge University Press, Cambridge

Freile D, Hillis L (1997) Carbonate productivity by *Halimeda incrassata* in a land proximal lagoon, Pico Feo, San Blas, Panama. Proc 8th Int Coral Reef Symp 1:767-772

Geister J (1977) The influence of wave exposure on the ecological zonation of Caribbean coral reefs. Proc 3rd Int Coral Reef Symp 2:23-29

Guisan, A, Zimmermann NE (2000) Predictive habitat distribution models in ecology. Ecol Model 135:147-186

Guinan J, Grehan AJ, Dolan MFJ, Brown C (2009) Quantifying relationships between video observations of cold-water coral cover and seafloor features in rockall trough, west of Ireland. Mar Ecol Prog Ser 375:125-138

Haining R (2003) Spatial data analysis: Theory and practice. Cambridge University Press, Cambridge

Hamylton S (2011) The use of remote sensing and linear wave theory to model local wave energy around Alphonse Atoll, Seychelles. Estuar Coast Shelf Sci 95:349-358

Hamylton S, Spencer T, Hagan A (2012) Spatial modelling of benthic cover using remote sensing data in the Aldabra lagoon, western Indian Ocean. Mar Ecol Prog Ser 460:35-47

Harney JN, Fletcher, CH (2003) A budget of carbonate framework and sediment production, Kailua Bay, Oahu, Hawaii. J Sediment Res 73:856-868

Hart DE, Kench PS (2007) Carbonate production of an emergent reef platform, Warraber Island, Torres Strait, Australia. Coral Reefs 26:53-68

Hearn CJ, Atkinson MJ, Falter JL (2001) A physical derivation of nutrient-uptake rates in coral reefs: effects of roughness and waves. Coral Reefs 20:347-356

Holthuijsen LH (2007) Waves in oceanic and coastal waters. Cambridge, UK: Cambridge University Press

Holthuijsen LH, Herman A, Booij N (2003) Phase-decoupled refraction-diffraction for spectral wave models. Coastal Engineering, 49:291-305.

Hopley D, Smithers S, Parnell K (2007) The geomorphology of the Great Barrier Reef: Development, diversity and change. Cambridge University Press, Cambridge

Hubbard DK, Miller AI, Scaturo D (1990) Production and cycling of calcium carbonate in a shelf-edge reef system (St. Croix, U.S. Virgin Islands); applications to the nature of reef systems in the fossil record. J Sediment Res 60:335-342

Hughes TP (1999) Off-reef transport of coral fragments at Lizard Island, Australia. Mar Geol 157:1-6

Kench P (2011) Eco-morphodynamics. In: Hopley, D (ed) Encyclopedia of modern coral reefs: Structure form and process. Springer, Berlin, pp 359-365

Kench P, Perry C, Spencer T (2009) Coral reefs. In: Slaymaker O, Spencer T, Embleton-Hamann C (eds) Geomorphology and global environmental change. Cambridge University Press, Cambridge, pp 180-213

Kendall M, Gibbons JD (1990) Rank correlation methods. Elsevier, New York

Kiene WS, Hutchings PA (1992) Long-term bioerosion of experimental coral substrates from Lizard Island, Great Barrier Reef. Proc 7th Int Coral Reef Symp 1:397-403

Kiene WS, Hutchings PA (1994) Bioerosion experiments at Lizard Island, Great Barrier Reef. Coral Reefs 13:91-98

Kinsey DW, Davies PJ (1975) Coral reef growth- A model based on morphological and metabolic studies. Aust J Mar Sci 7:10-14

Kinsey DW (1985) Metabolism, calcification and carbon production. Proc 5th Int Coral Reef Symp 1:527-539

Kinzie RA, Buddemeier RW (1996) Reefs happen. Global Change Biol 2:479-494

Kleypas JA, Langdon C (2006) Coral reefs and changing seawater carbonate chemistry. Coast Estuar Stud 61:73-110

Leon, JX, Woodroffe, C D (2013) Morphological characterisation of reef types in Torres Strait and an assessment of their carbonate production. Mar Geol, 338:64-75

Leon J, Phinn SR, Hamylton S, Saunders M (2013) Filling the ‘white ribbon’: A seamless multisource digital elevation / depth model for Lizard Island, northern Great Barrier Reef. Int J Remote Sens ‘in press’

LIMER Expedition Team (1975) Metabolic processes of coral reef communities at Lizard Island, Queensland. Search 7:463-468

Lugo-Fernandez CJ, Roberts H (2011) Reef front wave energy. In: Hopley, D (ed) Encyclopedia of modern coral reefs: Structure form and process. Springer, Berlin, pp 876-881

Lundblad E, Wright D, Miller J, Larkin E, Rinehart R, Naar D, Donahue B, Anderson S, Battista, T (2006) A Benthic Terrain Classification Scheme for American Samoa. Mar Geod 29:89-111

Macintyre IG, Glynn PW, Steneck RS (2001) A classic Caribbean algal ridge, Holandés Cays, Panamá: an algal coated storm deposit. Coral Reefs 20:95–105

Mallela J, Perry C (2007) Calcium carbonate budgets for two coral reefs affected by terrestrial runoff regimes, Rio Bueno, Jamaica. Coral Reefs 26:129–145

Massel SR (2005) Ocean surface waves: Their physics and prediction. Advanced Series on Ocean Engineering. World Scientific, Amsterdam

Montaggioni LF, Braithwaite CJR (2009) Quaternary coral reef systems: History, development, processes and controlling factors. Elsevier, Amsterdam

Moses CS, Andréfouët S, Kranenburg CJ, Muller-Karger FE (2009) Regional estimates of reef carbonate dynamics and productivity Using Landsat 7 ETM+, and potential impacts from ocean acidification. Mar Ecol Prog Ser 380:103-115

Nelson VM (1992) Patterns of cover, diversity and spatial arrangement of benthos at Lizard Island, Great Barrier Reef. Proc 7th Int Coral Reef Symp 1:827-832

Nielsen P (2009) Coastal and estuarine processes. World Scientific, Singapore

Perry CT, Edinger EN, Kench PS, Murphy GN, Smithers SG, Steneck RS, Mumby PJ (2012) Estimating rates of biologically driven coral reef framework production and erosion: a new census-based carbonate budget methodology and applications to the reefs of Bonaire. Coral Reefs 12:1-16

Pichon M, Morrissey J (1981) Benthic zonation and community structure of South Island reef, Lizard Island, Great Barrier Reef. Bull Mar Sci 31:581-593

Rees SA, Opdyke BN, Wilson PA, Keith Fifield L, Levchenko V (2006) Holocene evolution of the granite based Lizard Island and MacGillivray Reef systems, Northern Great Barrier Reef. Coral Reefs 25:555-565

Ris RC, Holthuijsen LH, Booij N (1999) A third-generation wave model for coastal regions 2. verification. Journal of Geophysical Research, 104:7667–7681

Sheppard CS, Dixon DJ, Gourlay M, Sheppard A, Payet R (2005) Coral mortality increases wave energy reaching shores protected by reef flats: Examples from the Seychelles. Estuar Coast Shelf Sci 64:223-234

Shinn EA (1966) Coral growth-rate, an environmental indicator. J Paleontol 40:233-240

Smirnov O, Anselin L (2001) Fast maximum likelihood estimation of very large spatial autoregressive models: a characteristic polynomial approach. Comput Stat Data Anal 35:301–319

Smith DF, Wiebe WJ (1977) Rates of carbon fixation, organic carbon release and translocation in a reef-building foraminifer, *Marginopora vevtebvalis*. Austral J Mar Freshw Res 28:311-319

Smith SV, Kinsey DW (1976) Calcium carbonate production, coral reef growth, and sea level change. Science 194:937-939

Trillobet A, Golubic S (2005) Cross-shelf differences in the pattern and pace of bioerosion of experimental carbonate substrates exposed for 3 years on the northern Great Barrier Reef, Australia. Coral Reefs 24:422-434

Van der Westhuysen AJ (2010) Modeling of depth-induced wave breaking under finite depth wave growth conditions. Journal of Geophysical Research, 115(C01008)

Vecsei A (2001) Fore-reef carbonate production: development of a regional census-based method and first estimates. Palaeogeogr Palaeoclimatol Palaeoecol 175:185-200

Vecsei A (2004) A new estimate of global reefal carbonate production including the forereefs. Global Planet Change 43:1-18

Veron JEN (2011) Corals: biology, skeletal deposition, and reef-building. In: Hopley D (ed) Encyclopedia of modern coral reefs: Structure form and process. Springer, Berlin, pp 275-281

Yamano H, Miyajima T, Koike I (2000) Importance of foraminifera for the formation and maintenance of a coral sand cay: Green Island, Australia. Coral Reefs 19:51-58

Zijlema M, van der Westhuysen, AJ (2005) On convergence behaviour and numerical accuracy in stationary SWAN simulations of nearshore wind wave spectra. Coastal Engineering, 52:237-256

List of Figures

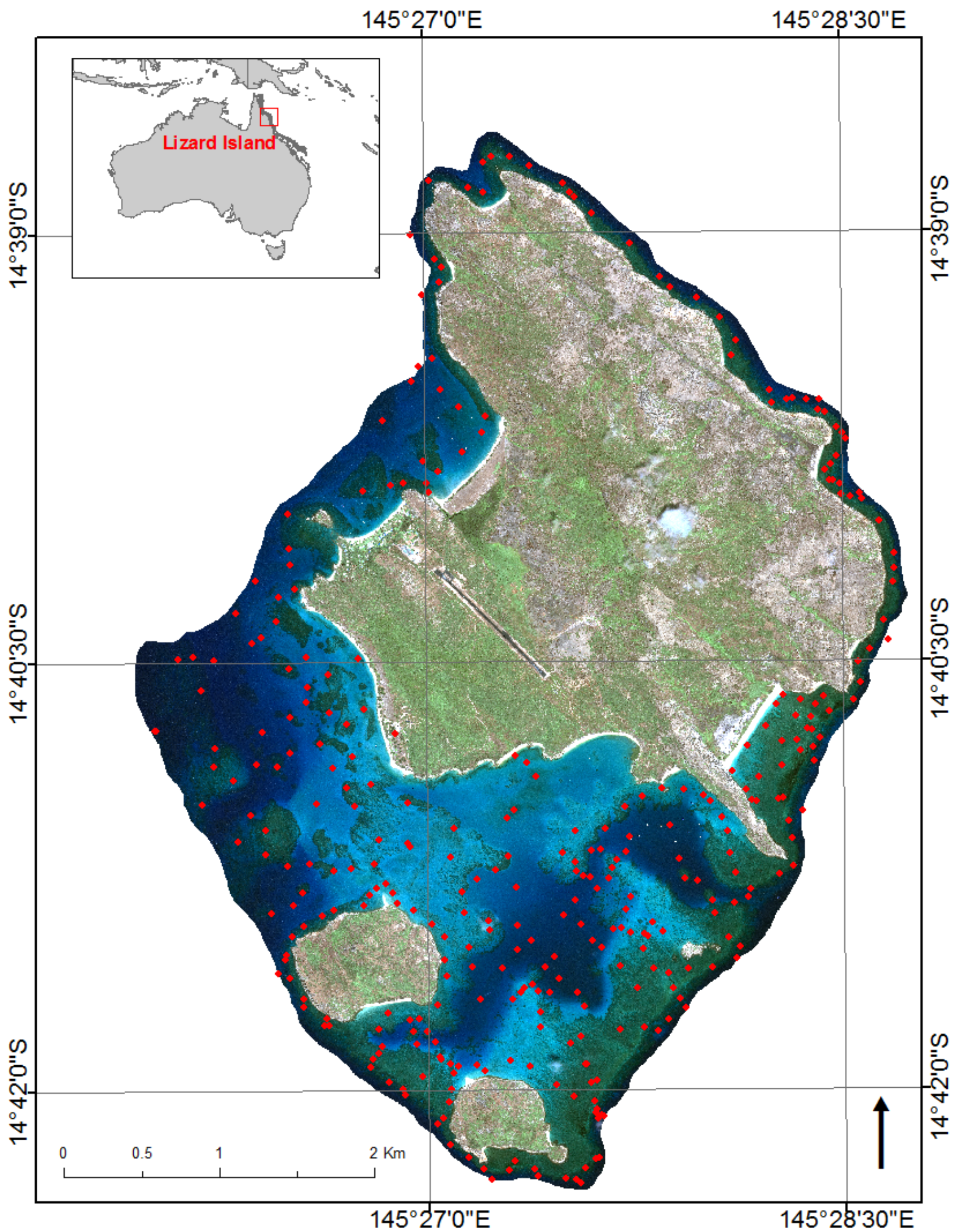

Figure 1. Lizard Island, Great Barrier Reef (145°27'145" E; 14°40'12" S). The red dots depict video ground referencing points. Inset: Location of Lizard Island along the Queensland coastline, Australia

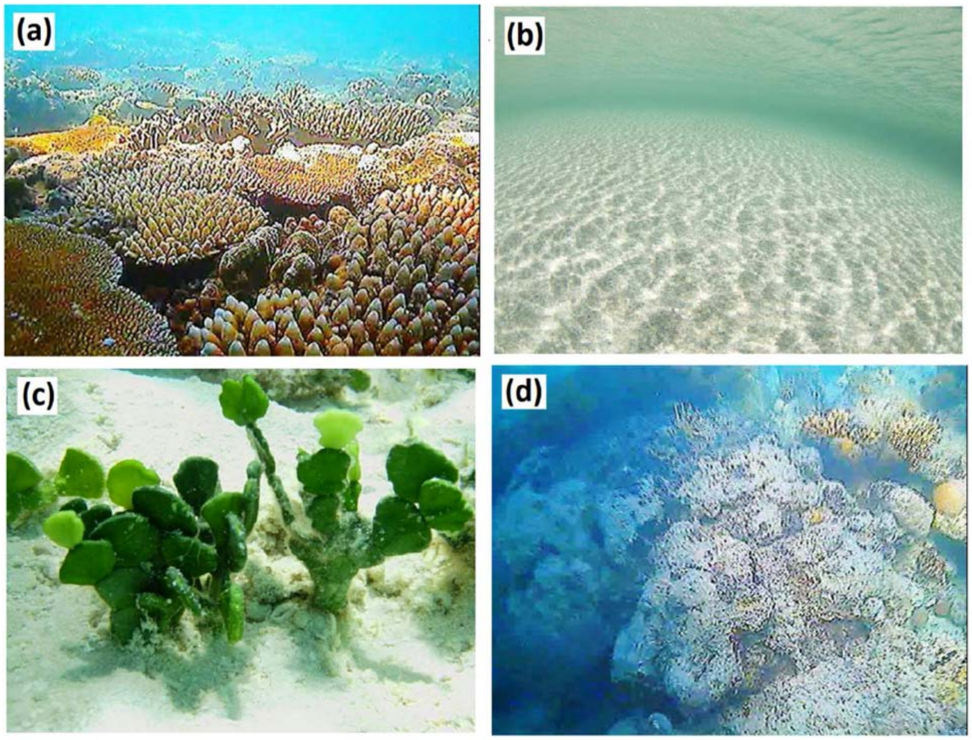

Figure 2. Key benthic carbonate producers at Lizard Island (a) live coral, (b) carbonate sand, (c) green calcareous macroalgae (*Halimeda*), and (d) encrusting calcified algae.

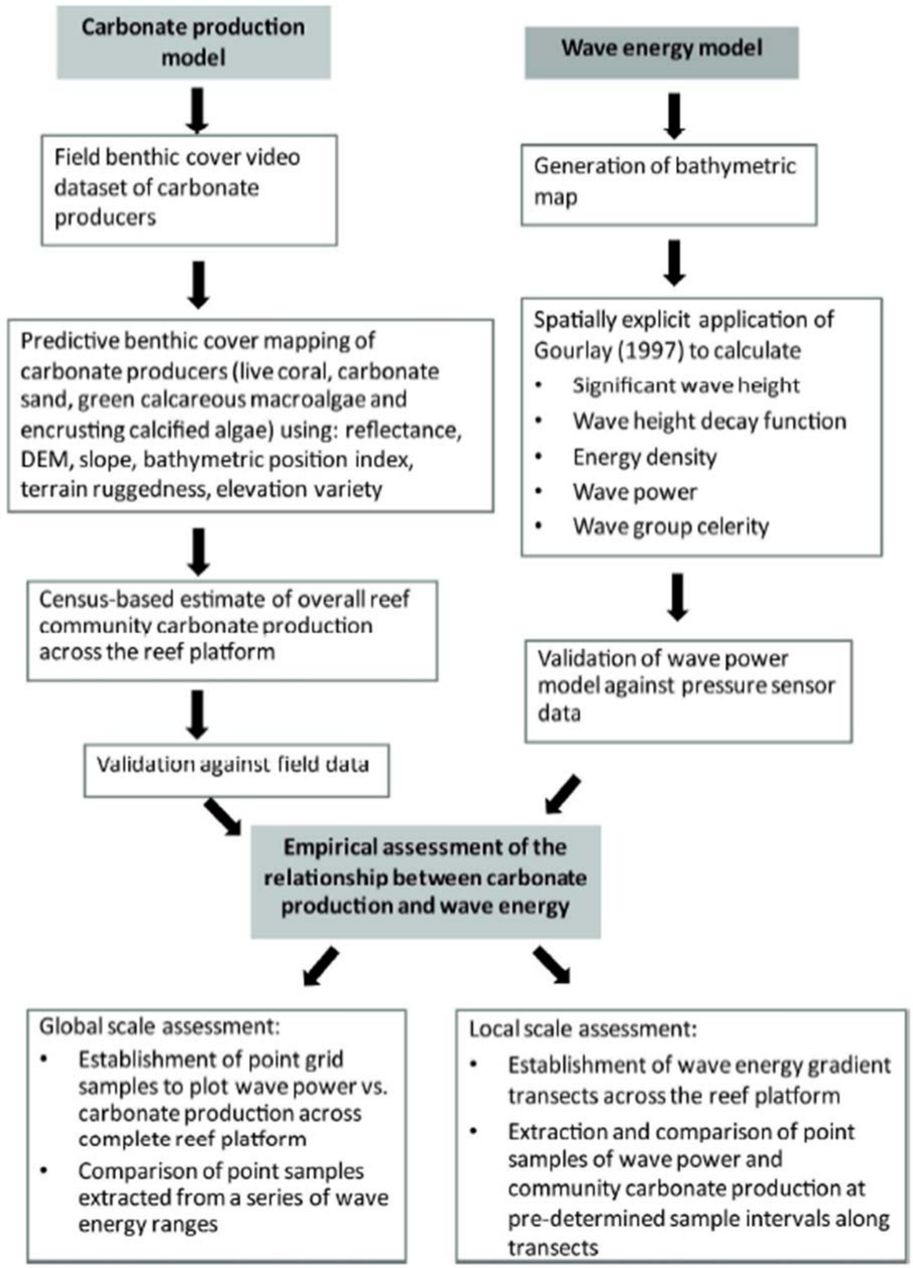

Figure 3. Schematic of the methodology for generating the carbonate production and wave energy models across the Lizard Island reef platform for the empirical assessment of the relationship between carbonate production and wave energy

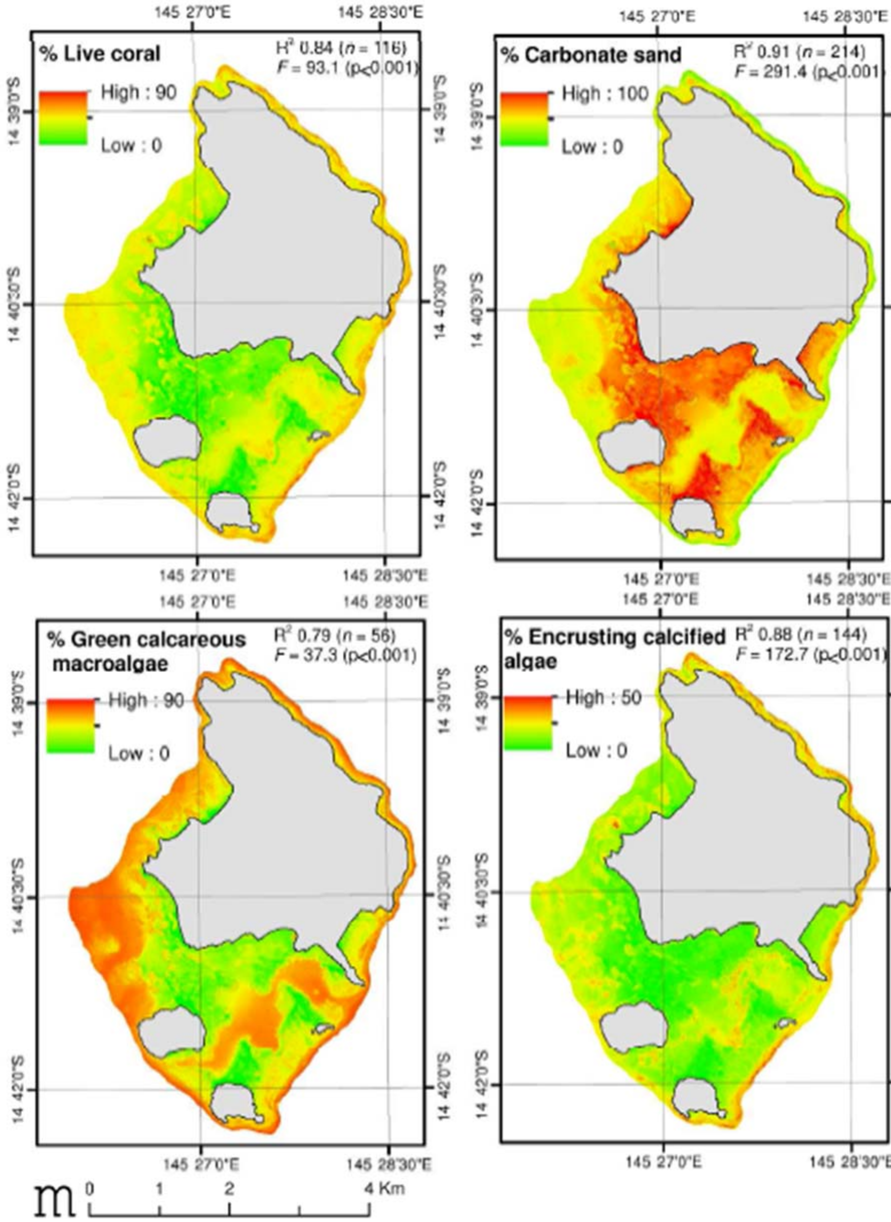

Figure 4 Predicted distribution models of each carbonate producing benthic component across the Lizard Island reef platform (*a* = live coral, *b* = carbonate sand, *c* = green calcareous macroalgae and *d* = encrusting calcified algae).

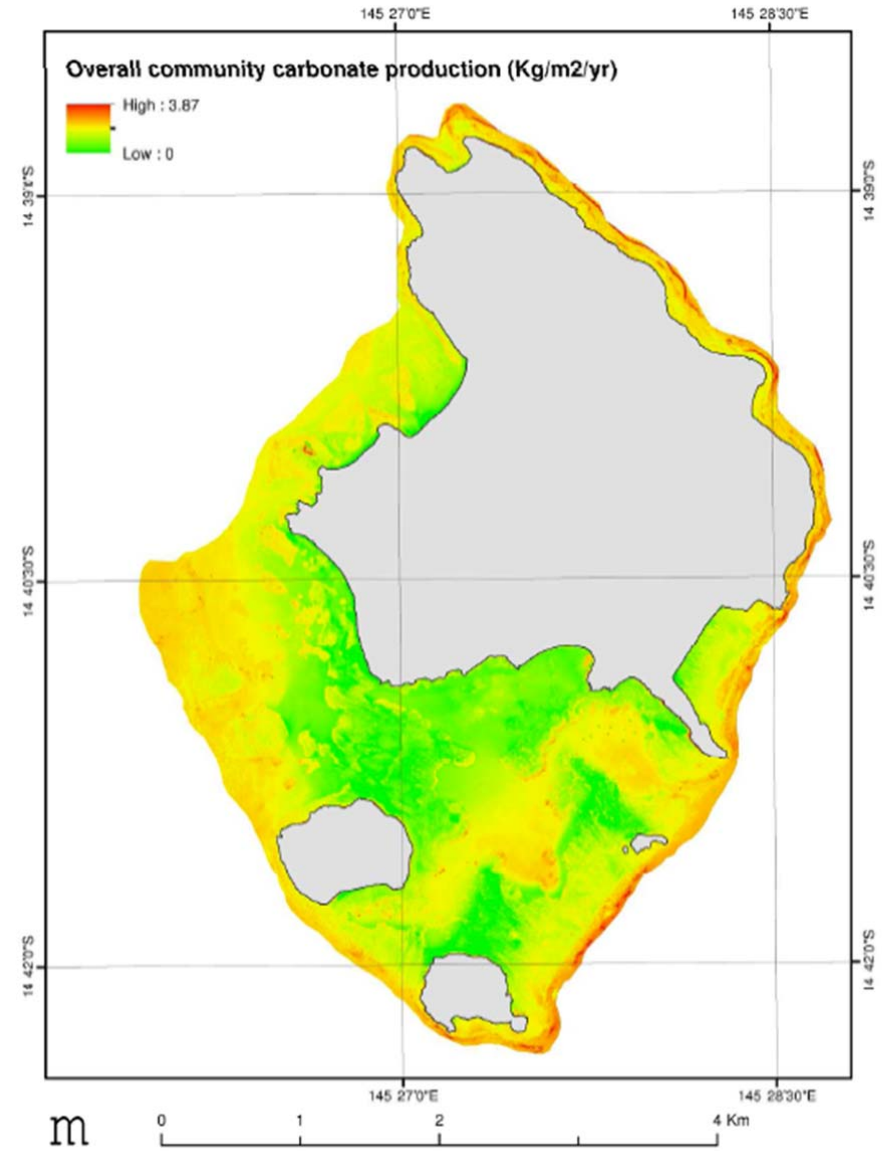

Figure 5 Modelled reef community calcium carbonate production across the Lizard Island reef platform.

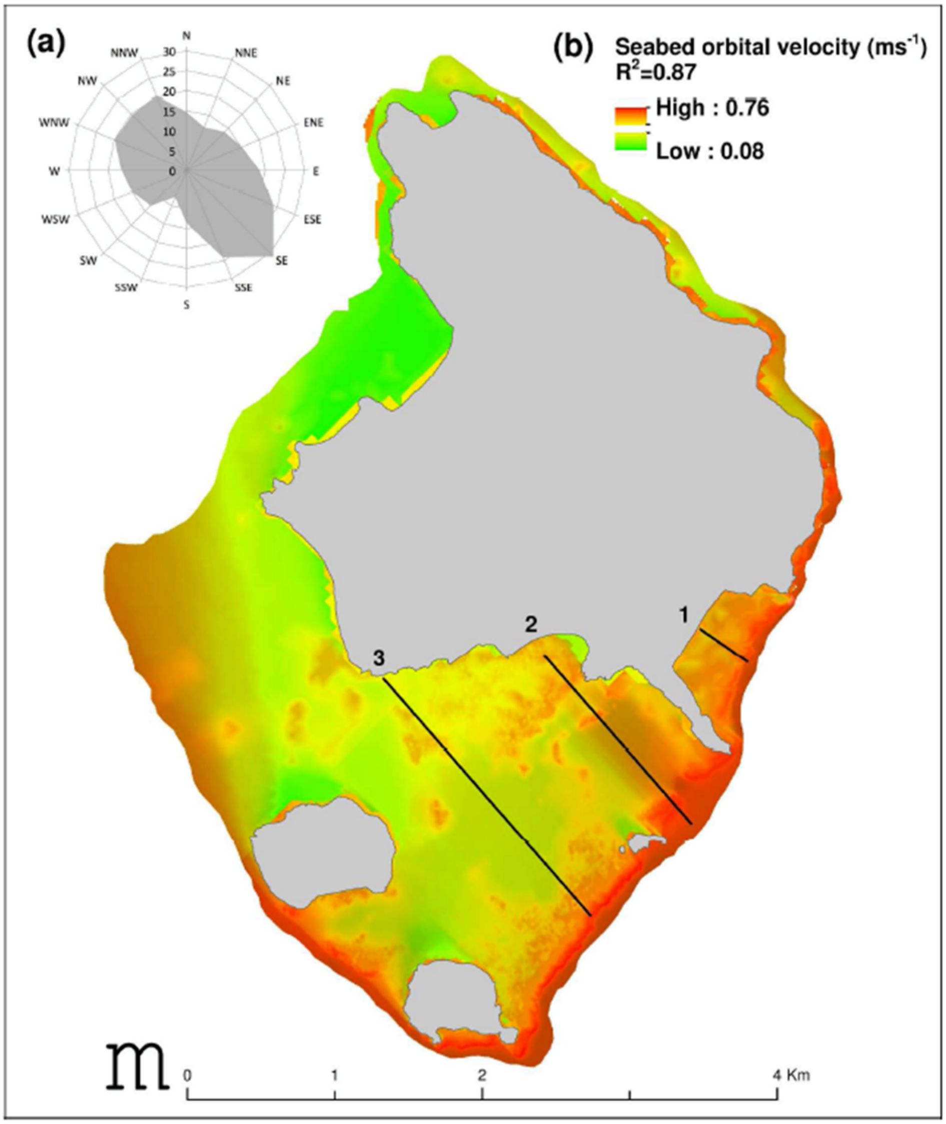

Figure 6 (a) Wind rose indicating incident wind fields generated from data collected from the Lizard Island weather station buoy AIMS Sensor network, August 2010 – October 2012 (b) modelled distribution of seabed orbital velocity across the Lizard Island reef platform generated from the SWAN model.

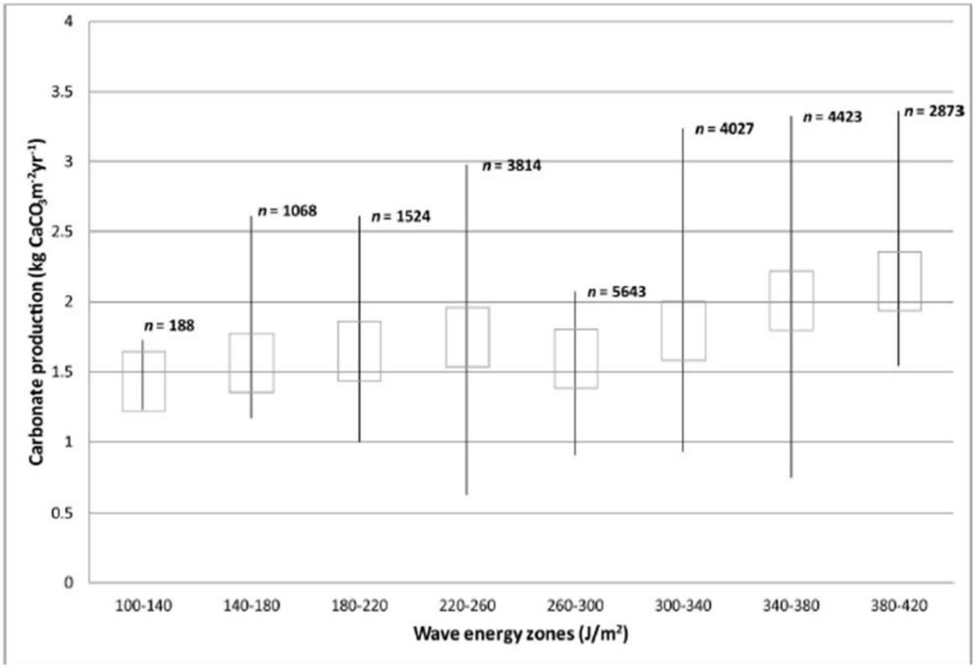

Figure 7 Box plot of carbonate production values of sample points extracted from eight different wave energy zones. Box extents represent cumulative error ranges, the mean is in the center of each box, lines represent the range of carbonate production and *n* equals the number of points extracted from each wave zone.

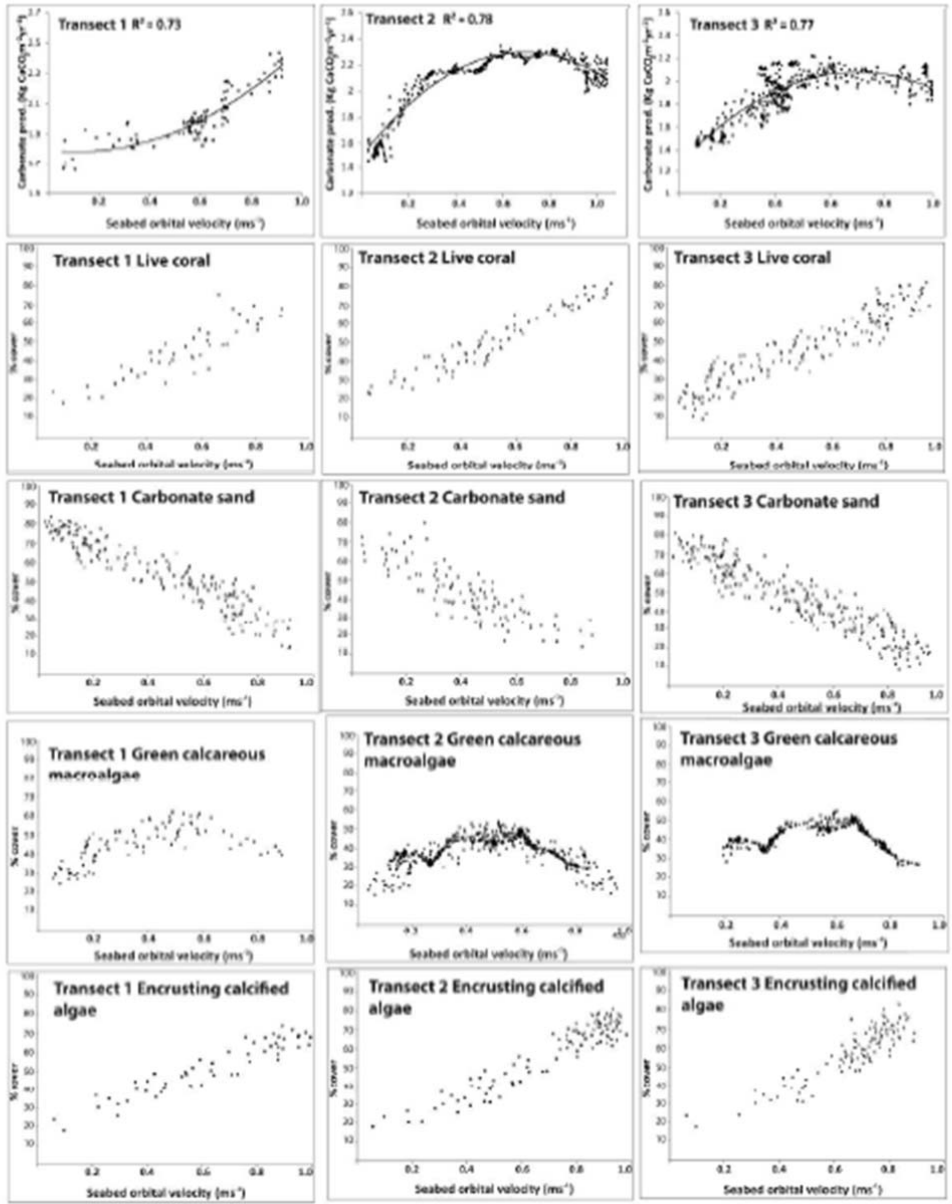

Figure 8 Row 1: Plots of total community carbonate production against seabed orbital velocity for values interrogated along transects 1 to 3 (see Figure 6 for transect locations). Rows 2-5 Plots of % cover of live coral, carbonate sand, green calcareous macroalgae and encrusting calcified algae against seabed orbital velocity for values interrogated along transects 1 to 3.

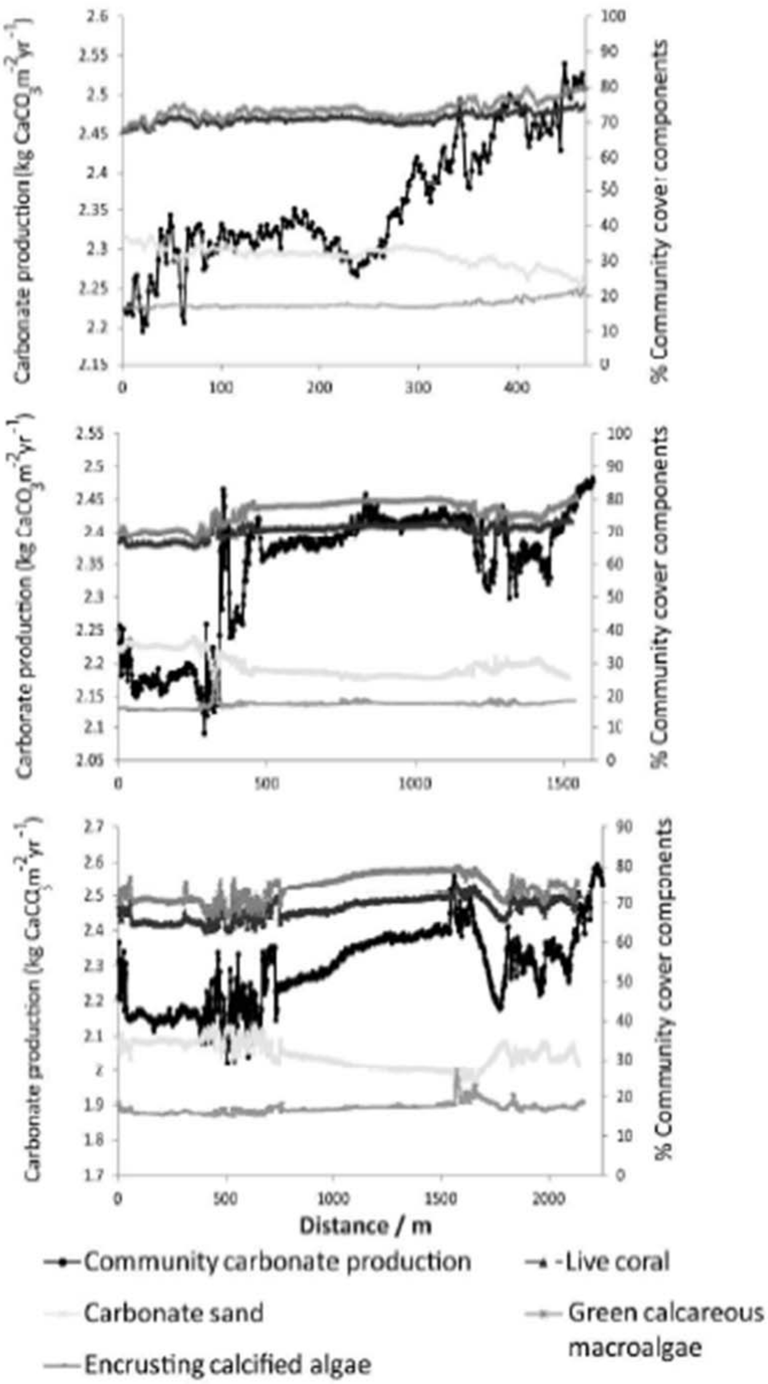

Figure 9 Local measures of total community carbonate production across three transects that traverse different geomorphological units of the reef platform at Lizard Island (black line, values indicated on the left hand vertical axis). % cover of individual community components contributing to carbonate production (live coral, carbonate sand, green calcareous macroalgae and encrusting calcified algae) along each transect (grey lines, normalized cover values indicated on the right hand vertical axis). Transect locations shown on the diagrams on the right hand side.